diffraction measurement revealed the formation of Li_2C_2 in the Li-doped CNT or graphite. We have also performed ultraviolet photoelectron spectroscopy (UPS) studies of valence band structure for both samples with and without Li. It was shown that the Li doping resulted in an extra half-filled electron-density-of-state containing the Fermi edge (*11*). The H_2-dissociative adsorption on carbon is a slow activated process (*12*), with an activation energy corresponding to an above-zero-energy crossing between the di-H atoms and H_2 molecular potential curves. Theoretical band-structure calculation (*13*) has indicated that the half-filled Fermi level band created by the Li doping can overlap strongly with the unoccupied antibonding H_2 $(1s^2)^*$ orbital, which to a large extent reduces the energy barrier for H_2 dissociation. We can therefore observe the high H_2 uptake resulting from Li doping.

The H_2-rechargeability of Li- and K-doped samples was tested by TGA. For Li-doped samples (CNT and graphite), the saturated H_2 uptake was measured at 653 K after each complete desorption at 823 K, whereas for K-doped carbon materials it was measured at 298 K after each run of desorption at 773 K. The results show that after more than 20 cycles of absorption-desorption, the capacities of H_2 uptake are reduced by less than 10% for both systems. High H_2 pressure was shown to favor the H_2 absorption, which is expected because H_2 uptake is a volume-reducing process. TPD measurements have demonstrated that the Li-doped CNT exposed to H_2 at 10 atm for 1 hour can store the same amount of H_2 as those systems at ambient pressure for 2 hours.

Although K-doped carbon samples can absorb H_2 at lower temperature than Li-doped samples, Li-doped carbon materials are chemically more stable than K-doped carbon materials. They can maintain H_2 uptake capability even after being heated in air at 373 K for hours, and no flame resulted even when the samples were exposed to air at 673 K after H_2 had been absorbed. On the other hand, K-doped CNT can be oxidized rapidly and even cause fire shortly after being exposed to air at room temperature. Nevertheless, both systems may find wide applications in the near future.

References and Notes

1. G. C. Carter and F. L Carter, *Metal-Hydrogen Systems*, T. Nejat Veziroglu, Ed. (Pergamon, Oxford, 1981), chap. 7.
2. H. Buchner, P. Pelloux-Gervais, M. Müller, F. Grafwallner, P. Luger, *Hygrogen and Other Alternative Fuels for Air and Ground Transportation*, H. W. Pohl, Ed. (Wiley, Chichester, UK, 1995), chaps. 7 to 11.
3. J. Nitsch, W. Peschka, W. Schnurnberger, M. Fischer, H. Eichert, in *Hydrogen as an Energy Carrier*, C. Winter and J. Nitsch, Eds. (Springer-Verlag, Berlin, 1988), part B.
4. S. Hynek, W. Füller, J. Bentley. *Int. J. Hydrogen Energy* **22**, 601 (1997).
5. A. C. Dillon, K. M. Jones, T. A. Bekkedahl, C. H. Kiang, D. S. Bethuune, M. J. Heben, *Nature*, **386**, 377 (1997).
6. A. Chambers, C. Park, R. T. K. Baker, *J. Phys. Chem. B* **102**, 4253 (1998).
7. Y. Ye *et al.*, *Appl. Phys. Lett.*, **74**, 2307 (1999).
8. P. Chen, X. Wu, J. Lin, K. L. Tan, *Phys. Rev. Lett.* **82**, 254 (1999); P. Chen, H. B. Zhang, G. D. Lin, Q. Hong, K. R. Tsai, *Carbon* **35**, 1495 (1997).
9. X. Wu, P. Chen, J. Lin, K. L. Tan, *Int. J. Hydrogen Energy*, in press.
10. R. M. Silverstein, G. C. Bassler, T. C. Morrill, *Spectrometric Identification of Organic Compounds* (Wiley, New York, 1991), pp. 103–107.
11. R. Schlagl, in *Progress in Intercalation* Research, W. Müller-Warmuth and R. Schollorn, Eds. (Kluwer, Dordrecht, Netherlands, 1994), pp. 83–176.
12. R. I. Masel, *Principles of Adsorption and Reaction on Solid Surfaces* (Wiley, New York, 1996), p. 443.
13. N. A. Holzwarth, S. Rabii, L. A. Girifalco, *Phys. Rev. B* **18**, 5190 (1978).

12 January 1999; accepted 1 June 1999

Regulation of NMDA Receptors by an Associated Phosphatase-Kinase Signaling Complex

Ryan S. Westphal,[1]* Steven J. Tavalin,[1]* Jerry W. Lin,[2] Neal M. Alto,[1] Iain D. C. Fraser,[1] Lorene K. Langeberg,[1] Morgan Sheng,[2] John D. Scott[1]†

Regulation of *N*-methyl-D-aspartate (NMDA) receptor activity by kinases and phosphatases contributes to the modulation of synaptic transmission. Targeting of these enzymes near the substrate is proposed to enhance phosphorylation-dependent modulation. Yotiao, an NMDA receptor–associated protein, bound the type I protein phosphatase (PP1) and the adenosine 3′,5′-monophosphate (cAMP)–dependent protein kinase (PKA) holoenzyme. Anchored PP1 was active, limiting channel activity, whereas PKA activation overcame constitutive PP1 activity and conferred rapid enhancement of NMDA receptor currents. Hence, yotiao is a scaffold protein that physically attaches PP1 and PKA to NMDA receptors to regulate channel activity.

The molecular organization of the postsynaptic density (PSD) is thought to be essential for the fidelity and precision of synaptic signaling events. Clustering and immobilization of neurotransmitter receptors and ion channels is maintained by an intricate system of protein-protein interactions (*1*). For example, NMDA receptors are clustered and coupled to the cytoskeleton through association with PDZ domain–containing proteins, α-actinin, and neurofilaments (*2*). Many signaling pathways converge on the NMDA receptor (*3*), allowing the regulation of channel activity in response to the generation of second messengers such as Ca^{2+} and cAMP (*4, 5*). PKA and PP1 activities modulate NMDA receptor function and appear to act in opposition to each other (*5, 6*). Individual targeting or anchoring proteins such as AKAP79 and spinophillin localize the kinase and phosphatase at the PSD (*7, 8*).

A two-hybrid screen for proteins that bind the NMDA receptor subunit isoform NR1A identified a protein called yotiao that interacts with the COOH-terminal C1 exon cassette of the ion channel (*9*). We isolated cDNAs encoding fragments of yotiao by an interaction cloning strategy to identify A-kinase anchoring proteins (AKAPs) (*10*) and confirmed that the protein bound NR1A (*11*). Expression of full-length yotiao fused to green fluorescent protein (GFP) in HEK 293 cells (*12*) resulted in detection of a ~210-kD protein that bound the type II regulatory subunit of PKA (RII), as assessed by overlay assay (Fig. 1A). Immunoprecipitations with antiserum to yotiao from brain extracts also isolated an RII binding protein and were enriched by a factor of 10.5 ± 2 (n = 3) for PKA catalytic subunit activity (Fig. 1, B and C). We mapped the RII binding site to a region between residues 1229 and 1480 by screening a family of recombinant yotiao fragments (Fig. 1D) in the overlay assay (Fig. 1, E and F). Residues 1440 to 1457 appear to include the principal determinants for RII interaction because a synthetic peptide encompassing this region blocked RII binding (Fig. 1F). These findings indicate that yotiao functions to anchor PKA to NMDA receptors.

Because PP1 activity participates in the regulation of NMDA receptors (*6*), we conducted experiments to address whether the

[1]Howard Hughes Medical Institute, Vollum Institute, Oregon Health Sciences University, 3181 S.W. Sam Jackson Road, Portland, OR 97201, USA. [2]Howard Hughes Medical Institute and Department of Neurobiology, Massachusetts General Hospital and Harvard Medical School, Boston, MA 02114, USA.

*These authors contributed equally to this article.
†To whom correspondence should be addressed. E-mail: scott@ohsu.edu

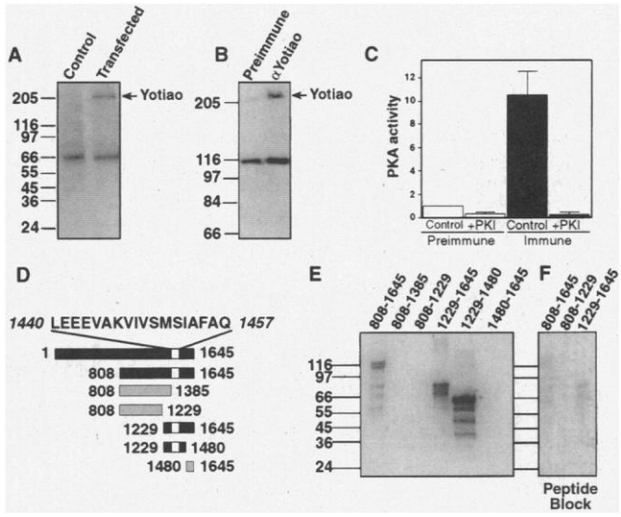

Fig. 1. Identification of yotiao as an AKAP. (**A**) Binding of full-length yotiao to RII. Lysates prepared from HEK 293 cells transfected with control vector or a yotiao-GFP fusion construct (*12*) were subjected to RII overlay assay as described (*23*). (**B**) Immunoprecipitation of yotiao. Preimmune or immune (αYotiao) sera were used for immunoprecipitation from rat brain extracts as described (*24*). Immunoprecipitated complexes were blotted and subjected to RII overlay assay (*23*). (**C**) Coprecipitation of PKA activity with yotiao immune sera. Immunoprecipitated material from rat brain extracts was incubated with cAMP (10 mM) and assayed for kinase activity (*24*) in the absence (control) and presence (+PKI) of 4 μM PKA inhibitor PKI (*15*). Values show activity relative to that associated with preimmune serum and are expressed as means ± SEM of three separate experiments. (**D**) Schematic representation of recombinant yotiao fragments (*25*). Abbreviations for amino acid residues: A, Ala; E, Glu; F, Phe; I, Ile; K, Lys; L, Leu; M, Met; Q, Gln; S, Ser; and V, Val. (**E** and **F**) Mapping of the RII binding domain on yotiao. Fragments of yotiao were blotted and assayed for RII binding by overlay assay in the absence (E) and presence (F) of a yotiao peptide encompassing residues 1440 to 1457 (10 μM). Equal amounts of protein were present in each lane, as determined by staining of protein on the membrane. Relative molecular mass standards (in kilodaltons) are at the left in (A), (B), and (E).

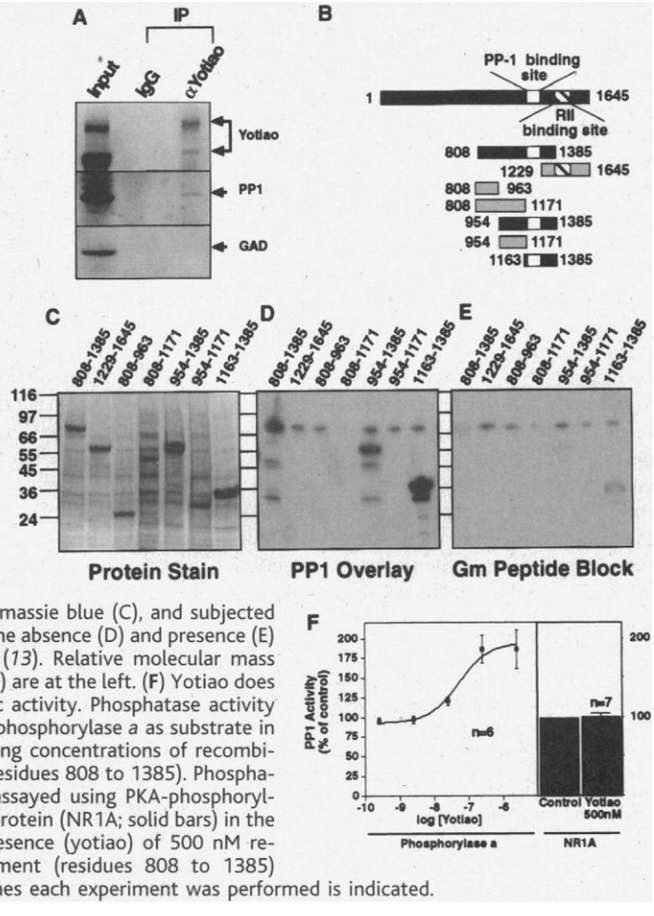

Fig. 2. PP1 targeting by yotiao. (**A**) Coimmunoprecipitation of PP1 with yotiao. Immunoprecipitations from rat brain extracts were done as described (*24*) with affinity-purified antibodies to yotiao or control immunoglobulin G (IgG). Precipitates were blotted and probed with antibodies to PP1, glutamic acid decarboxylase (GAD), or yotiao (*26*). (**B**) Schematic representation of recombinant yotiao fragments (*25*). (**C** to **E**) Direct interaction of PP1 with yotiao in overlay assays. Bacterial extracts expressing recombinant fragments of yotiao were separated by SDS-PAGE, transferred to a membrane, stained with Coomassie blue (C), and subjected to PP1 overlays (*26*) in the absence (D) and presence (E) of 10 μM Gm peptide (*13*). Relative molecular mass standards (in kilodaltons) are at the left. (**F**) Yotiao does not inhibit PP1 catalytic activity. Phosphatase activity was assayed (*27*) using phosphorylase *a* as substrate in the presence of increasing concentrations of recombinant yotiao fragment (residues 808 to 1385). Phosphatase activity was also assayed using PKA-phosphorylated GST-NR1A fusion protein (NR1A; solid bars) in the absence (control) or presence (yotiao) of 500 nM recombinant yotiao fragment (residues 808 to 1385) (*27*). The number of times each experiment was performed is indicated.

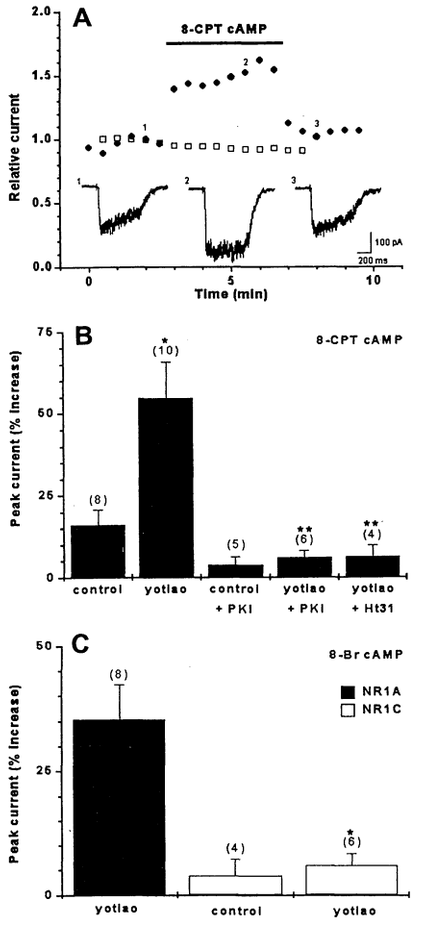

Fig. 3. Facilitation by yotiao of cAMP-dependent modulation of recombinant NMDA receptor currents. (**A**) Whole-cell recordings from HEK 293 cells expressing heteromeric NMDA receptors consisting of NR1A and NR2A (*14*). Currents were evoked every 30 s by 500-ms applications of glutamate (1 mM) in the presence of glycine (100 μM). Examples of the time course for modulation of recombinant NMDA receptor currents by the cell-permeant cAMP analog 8-CPT cAMP are shown for a cell in which yotiao was expressed (solid circles) and a control cell (open squares). Currents were normalized to the peak of the first sweep recorded from each cell. Representative traces are included from a yotiao-expressing cell (1) before, (2) during, and (3) after 8-CPT cAMP treatment. (**B**) Bar graph of the percent increases in peak whole-cell current from control cells, yotiao-expressing cells, yotiao-expressing cells in the presence of PKI peptide (10 μM), and yotiao-expressing cells in the presence of Ht31 peptide (10 μM) upon application of 8-CPT cAMP. Significant differences (*$P < 0.01$ compared to control; **$P < 0.01$ compared to yotiao) and the number of times each experiment was performed are indicated. (**C**) Bar graph of the percent increases in peak whole-cell current in response to application of 8-bromo-cAMP (8-Br cAMP; 100 μM). Solid bar, cells expressing NR1A; open bars, cells expressing NR1C. Expression of yotiao is indicated. Significant differences (*$P < 0.01$ compared to NR1A) and the number of times each experiment was performed are indicated.

phosphatase also associated with yotiao. Immunoprecipitation of yotiao from brain extracts resulted in the copurification of PP1 (Fig. 2A). In overlay assays, PP1 bound to recombinant fragments (Fig. 2B) expressed in *Escherichia coli* (Fig. 2C) encompassing residues 1171 to 1229 of yotiao (Fig. 2, C and D) and the PP1 targeting inhibitor peptide Gm (*13*) blocked PP1 binding to yotiao (Fig. 2E). A hallmark of some PPI targeting subunits is the presence of a Lys-Val-X-Phe (KVXF) motif that binds to an allosteric site on the catalytic subunit of the phosphatase (*13*). Although yotiao contains this motif, it is not essential for interaction between yotiao and PP1. Binding of yotiao had no effect on PP1 activity toward an NR1A receptor fragment, and it enhanced activity by a factor of 1.9 ± 0.2 ($n = 6$) toward phosphorylase *a* with a median effective concentration (EC_{50}) of 52 nM (Fig. 2F). These results show that yotiao is not an inhibitor of PP1 activity, hence yotiao may target active PP1 to the NMDA receptor.

Currents through NMDA receptors are enhanced after activation of PKA (*5*) or inhibition of PP1 (*6*). We made whole-cell recordings of transfected HEK 293 cells (*14*) that expressed NMDA receptors alone or NMDA receptors and yotiao. Application of the cell-permeant cAMP analog 8-(4-chlorophenylthio)-cAMP (8-CPT cAMP) enhanced NMDA currents to a greater extent in cells expressing yotiao ($54.9 \pm 11.0\%$; $n = 10$; $P < 0.01$) than in control cells ($16.1 \pm 4.6\%$; $n = 8$) (Fig. 3, A and B). The effect of cAMP was inhibited by introduction of the PKA inhibitor peptide PKI 5-24 (*15*) or the RII anchoring inhibitor peptide Ht31 (*16*) through the patch pipette. These results indicate that an anchored pool of PKA was required for augmentation of the current (Fig. 3B).

Yotiao did not facilitate the cAMP-dependent modulation of NMDA receptors containing the NR1C subunit, which lacks the C1 exon (Fig. 3C). This suggests that yotiao selectively regulates NMDA receptors containing the C1 exon.

To test for a role of yotiao-dependent anchoring of PP1 in the modulation of NMDA receptor activity, we dialyzed Gm peptide into cells through the patch pipette. A significantly greater time-dependent increase in NMDA receptor currents ($41.1 \pm 10.2\%$; $n = 7$; $P < 0.01$) was observed in yotiao-expressing cells relative to control cells ($9.0 \pm 3.6\%$; $n = 7$). The effect of the inhibitor plateaued within 5 to 10 min of establishing the whole-cell configuration, whereas no effect was observed with NMDA receptors containing NR1C (Fig. 4). Application of the phosphatase inhibitor okadaic acid at 1 μM (but not 10 nM) produced an effect similar to that of Gm peptide on NR1A in yotiao-expressing cells ($28.5 \pm 3.6\%$; $n = 4$; $P < 0.05$) relative to control cells ($2.3 \pm 6.9\%$; $n = 4$) (Fig. 4B). These results indicate that tonic PP1 activity associated with yotiao may negatively regulate NMDA receptors. The extent of the increase in current conducted by the NMDA receptor was related to the initial extent of current desensitization (*17*). This relation was observed whether we activated PKA or displaced PP1. Thus, yotiao-mediated localization of PKA and PP1, the balance of enzyme activities, and the initial state of the channel all appear to contribute to the modulation of current flow through the NMDA receptor.

Under resting conditions, targeting of a constitutively active phosphatase may favor dephosphorylation of the channel or a closely associated protein. However, when intracellular concentrations of cAMP are increased, PKA may be released from anchored sites, thus shifting the equilibrium in favor of phosphorylation, which in turn results in enhancement of current flow through the NMDA receptor.

Subcellular targeting of phosphatases and kinases is achieved through various mechanisms. Sometimes both enzymes interact with each other (*18*), but complex formation more often requires an intermediary protein (*19*). Scaffold proteins such as sterile 5, Pbs-2, and Jip-1 immobilize successive members in a kinase cascade such that signals can be efficiently transduced from one kinase to the next (*20*). In contrast, multivalent scaffold proteins such as AKAP79, PTG, and InaD coordinate the location of several signaling enzymes and thus integrate diverse signals at a specific intracellular site (*7, 21*). Yotiao facilitates the dynamic regulation of an individual phosphoprotein by assembling a signaling complex that contains a kinase and phosphatase with opposing activities and is attached to the substrate. Interestingly, the gene encoding yotiao is alternatively spliced to yield a family of proteins, including the recently identified AKAP350. This splice variant of yotiao also contains the interaction domains for PP1, NR1A, and PKA and therefore may also mediate the assembly of a macromolecular complex involved in regulating NMDA receptor function. Because a number of ion channels appear to be modulated by closely associated kinases and phosphatases (*22*), other structural elements similar to yotiao may exist.

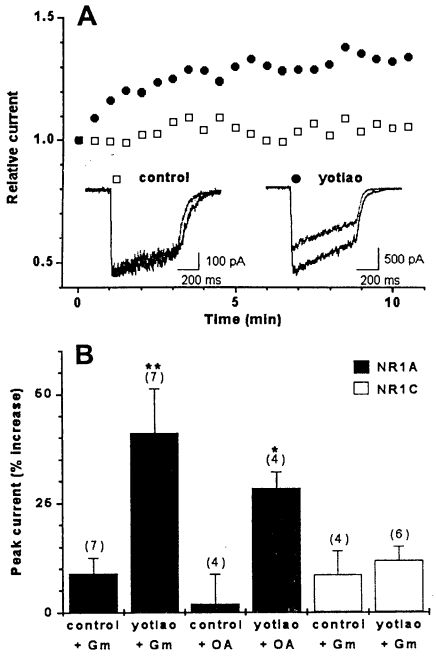

Fig. 4. Influence of yotiao on regulation of NMDA receptor activity by PP1 activity. **(A)** Time course of normalized peak NMDA receptor currents from a control and yotiao-expressing cell during whole-cell dialysis of Gm peptide (10 μM). Traces shown below correspond to the first and last sweep from the indicated cells after establishment of the whole-cell configuration. **(B)** Bar graph summarizing percent increase of peak whole-cell current for cells expressing NR1A (solid bars) and cells expressing NR1C (open bars). Expression of yotiao and the use of Gm or okadaic acid (OA, 1 μM) are indicated. Significant differences (**$P < 0.01$, *$P < 0.05$) and the number of times each experiment was performed are indicated.

References and Notes

1. E. B. Ziff, *Neuron* **19**, 1163 (1997); M. Sheng, *ibid.* **17**, 575 (1996); S. E. Craven and D. S. Bredt, *Cell* **93**, 495 (1998); M. B. Kennedy, *Trends Neurosci.* **20**, 264 (1997).
2. H.-C. Kornau, L. T. Schenker, M. B. Kennedy, P. H. Seeburg, *Science* **269**, 1737 (1995); M. Niethammer *et al.*, *Neuron* **20**, 693 (1998); J. E. Brenman *et al.*, *J. Neurosci.* **18**, 8805 (1998); M. Wyszynski *et al.*, *Nature* **385**, 439 (1997); M. D. Ehlers *et al.*, *J. Neurosci.* **18**, 720 (1998).
3. W. G. Tingley *et al.*, *Nature* **364**, 70 (1993); L. Chen and L. Y. M. Huang, *ibid.* **356**, 521 (1992); Y. T. Wang and M. W. Salter, *ibid.* **369**, 233 (1994); M. D. Ehlers, W. G. Tingley, R. L. Huganir, *Science* **269**, 1734 (1995).
4. C. Rosenmund and G. L. Westbrook, *Neuron* **10**, 805 (1993); S. Zhang *et al.*, *ibid.* **21**, 443 (1998); D. N. Lieberman and I. Mody, *Nature* **369**, 235 (1994); G. Tong, D. Shepherd, C. E. Jahr, *Science* **267**, 1510 (1995).
5. I. M. Raman, G. Tong, C. E. Jahr, *Neuron* **16**, 415 (1996); R. Cerne, K. I. Rusin, M. Randic, *Neurosci. Lett.* **161**, 124 (1993).
6. L. Y. Wang, B. A. Orser, D. L. Brautigan, J. F. MacDonald, *Nature* **369**, 230 (1994); T. Blank *et al.*, *Proc. Natl. Acad. Sci. U.S.A.* **94**, 14853 (1997); G. L. Snyder, A. A. Fienberg, R. L. Huganir, P. Greengard, *J. Neurosci.* **18**, 10297 (1998).
7. T. M. Klauck *et al.*, *Science* **271**, 1589 (1996).
8. P. B. Allen, C. C. Ouimet, P. Greengard, *Proc. Natl. Acad. Sci. U.S.A.* **94**, 9956 (1997).
9. J. W. Lin *et al.*, *J. Neurosci.* **18**, 2017 (1998).
10. A rat pituitary λZAP cDNA expression library was screened with [^{32}P]-labeled RIIα as a probe [Z. E. Hausken, V. M. Coghlan, J. D. Scott, *Protein Targeting Protocols* (Humana, Totowa, NJ, 1996)] and a 2423–base pair (bp) cDNA clone, originally called GH415, was isolated. The 5′ end of GH415 and other clones isolated from brain cDNA libraries exhibited homology to yotiao (*6*). Nucleotide database searches using the National Center for Biotechnology Information basic local alignment search tool (BLAST), and isolation of additional clones, demonstrated that yotiao belongs to an alternatively spliced family of AKAPs that lie on chromosome 7q21 and include a previously identified AKAP fragment, which contains its own RII binding domain, denoted as AKAP120 [D. T. Dransfield *et al.*, *Biochem. J.* **322**, 801 (1997)]. AKAP120 represents a larger protein [P. H. Schmidt *et al.*, *J. Biol. Chem.* **274**, 3055 (1999)]. To construct a yotiao-GFP expression vector, we generated the entire coding region (nucleotides 131 to 5169) by reverse transcription of human brain polyadenylated RNA with an oligonucleotide to the 3′ end of yotiao.

The 5038-bp fragment was amplified by the polymerase chain reaction (PCR) (Pfu turbo polymerase, Stratagene), sequenced, and inserted into the mammalian expression vector pEGFP.

11. Glutathione S-transferase (GST) fusions of an NR1A fragment (residues 834 to 935) or an NR1C fragment (residues 834 to 898) were incubated for 4 hours at 4°C with HEK 293 cell lysates expressing yotiao. Complexes were isolated by affinity chromatography on glutathione-agarose and were separated by SDS–polyacrylamide gel electrophoresis (PAGE) (4 to 15% gel). Yotiao immunoreactivity was enriched in samples incubated with the GST-NR1A fusion protein but not in samples incubated with the corresponding region of NR1C.
12. HEK 293 cells (10-cm dishes) were transfected with pEGFP (20 μg) or yotiao-GFP (20 μg) by the calcium phosphate method [C. Chen and H. Okayama, *Mol. Cell. Biol.* **7**, 2745 (1987)].
13. The phosphatase blocking peptide consisted of residues 63 to 75 (Gly-Arg-Arg-Val-Ser-Phe-Ala-Asp-Asn-Phe-Gly-Phe-Asn) of the muscle form of the PP1 regulatory G subunit [D. F. Johnson *et al.*, *Eur. J. Biochem.* **239**, 317 (1996)]. This sequence contains the KVXF motif that binds to an allosteric site on PP1C [M. P. Egloff *et al.*, *EMBO J.* **16**, 1876 (1997)].
14. HEK 293 cells plated at low density (~50,000 cells) on 35-mm culture dishes (Falcon) were transfected with 1 μg each of cDNA encoding NR1A, NR2A, CD4 cell surface marker, and yotiao-GFP construct (10 μg) by the calcium phosphate method (*12*). Twenty-four hours after transfection, cells were visually selected by adherence of CD4 antibody–coated beads and GFP epifluorescence. Whole-cell recordings [O. P. Hamill *et al.*, *Pfluegers Arch.* **391**, 85 (1981)] were made with an Axopatch 200B amplifier (Axon Instruments). Patch pipettes (2 to 4 megohms) contained 140 mM Cs methanesulfonate, 10 mM Hepes (pH 7.4), 5 mM adenosine triphosphate (Na salt), 10 mM 1,2-bis(2-aminophenoxy)ethane-*N*,*N*,*N*′,*N*′-tetraacetic acid, and 5 mM $MgCl_2$. Peptides were added to the pipette solution from frozen concentrated stocks. Extracellular solution contained 140 mM NaCl, 5 mM KCl, 1.8 mM $CaCl_2$, 10 mM Na-Hepes (pH 7.4), 10 mM glucose, and 100 μM glycine. Glutamate and cAMP analogs were added from frozen stocks. Rapid solution exchanges were accomplished through a series of flow pipes mounted onto a piezoelectric bimorph to evoke NMDA receptor currents. Cells were lifted off the bottom of the dish to speed the solution exchange time. Currents were digitized at 5 kHz and filtered at 1 kHz with a Digidata 1200B board and Clampex 7 software (Axon Instruments). Series resistance (90 to 95%) and whole-cell capacitance compensation were used. All experiments were done at a holding potential of −60 mV at room temperature. No differences in current amplitudes were detected from control and yotiao-transfected cells (range of 100 pA to 12 nA for both). This variability most likely reflects differences in transfection efficiency. Data are expressed as means ± SEM.
15. J. D. Scott *et al.*, *Proc. Natl. Acad. Sci. U.S.A.* **82**, 4379 (1985).
16. D. W. Carr *et al.*, *J. Biol. Chem.* **267**, 13376 (1992); C. Rosenmund *et al.*, *Nature* **368**, 853 (1994).
17. Desensitization was quantified as the ratio of current remaining at the end of a 500-ms application of glutamate to the peak current. Under our recording conditions, glycine-independent desensitization was the only form of desensitization or inactivation observed [R. A. Lester, G. Tong, C. E. Jahr, *J. Neurosci.* **13**, 1088 (1993); J. J. Krupp, B. Vissel, S. H. Heinemann, G. L. Westbrook, *Mol. Pharmacol.* **50**, 1680 (1996)]. This property of the receptor is regulated by phosphorylation [G. Tong and C. E. Jahr, *J. Neurophysiol.* **72**, 754 (1994)]. Therefore, the extent of desensitization may reflect the phosphorylation state of the receptor or closely associated protein. Non-desensitizing receptors may be highly phosphorylated and less likely to undergo further phosphorylation. Strongly desensitizing currents may arise from largely dephosphorylated receptors, which can then be activated by phosphorylation. Cells that had greater desensitization also had larger increases in current in response to cAMP analogs or Gm peptide.
18. R. S. Westphal, K. A. Anderson, A. R. Means, B. E. Wadzinski, *Science* **280**, 1258 (1998); M. Camps *et al.*, *ibid.*, p. 1262.
19. T. Pawson and J. D. Scott, *ibid.* **278**, 2075 (1997); D. Mochly-Rosen, *ibid.* **268**, 247 (1995).
20. F. Posas and H. Saito, *ibid.* **276**, 1702 (1997); K.-Y. Choi *et al.*, *Cell* **78**, 499 (1994); A. J. Whitmarsh, J. Cavanagh, C. Tournier, J. Yasuda, R. J. Davis, *Science* **281**, 1671 (1998).
21. J. A. Printen, M. J. Brady, A. R. Saltiel, *Science* **275**, 1475 (1997); S. Tsunoda *et al.*, *Nature* **388**, 243 (1997).
22. P. H. Reinhart and I. B. Levitan, *J. Neurosci.* **15**, 4572 (1995); G. F. Wilson, N. S. Magoski, L. K. Kaczmarek, *Proc. Natl. Acad. Sci. U.S.A.* **95**, 10938 (1998).
23. S. M. Lohmann, P. De Camilli, I. Elnig, U. Walter, *Proc. Natl. Acad. Sci. U.S.A.* **81**, 6723 (1984).
24. Rat brain extracts were prepared by Dounce homogenization of frozen brains in phosphate-buffered saline (PBS) containing 1 mM EDTA, 1 mM EGTA, 1 mM 4-(2-aminoethyl)-benzenesulfonyl fluoride, 1 mM benzamidine, pepstatin (2 μg/ml), and leupeptin (2 μg/ml), followed by centrifugation at 40,000*g* for 1 hour. Supernatant (1 ml) was incubated with 20 μl of preimmune or immune serum overnight at 4°C. After addition of protein G–agarose (30 μl) for 1 hour at 4°C, the precipitated complexes were washed five times with homogenization buffer and proteins were eluted with 2× SDS sample buffer. Yotiao was detected by RII overlay. For detection of PKA C subunit activity, immune complexes were incubated with 10 mM cAMP. PKA activity was measured with the substrate Kemptide as described [J. D. Corbin and E. M. Reimann, *Methods Enzymol.* **38**, 287 (1974)]. PKA activity was defined as the activity inhibited by the PKI 5-24 inhibitor peptide (*15*). Immunoprecipitations in Fig. 2 were performed as described [J. Luo *et al.*, *Mol. Pharmacol.* **51**, 79 (1997)].
25. Designated fragments of yotiao were amplified by PCR and subcloned into pGEX-4T3 (Amersham Pharmacia Biotech) or pet30b (Novagen). Inserted sequences were confirmed by DNA sequencing. GST fusion proteins were purified from bacterial extracts by affinity purification with glutathione-agarose (Amersham Pharmacia Biotech).
26. Bacterial extracts expressing fragments of yotiao as histidine-tagged fusion proteins were separated by SDS-PAGE (4 to 15% gels), transferred to polyvinylidene fluoride membranes (Millipore), and blocked overnight in 1% BLOTTO (5% nonfat dry milk, 1% bovine serum albumin, 25 mM tris, and 150 mM NaCl). Blots were then incubated with recombinant PP1 (2 μg/ml) for 2 hours, washed, and incubated with PP1 antisera (1:10,000) for 1 hour. After washing, blots were incubated with horseradish peroxidase–conjugated secondary antibody and washed. PP1 binding was detected by enhanced chemiluminescence (Pierce). Under these conditions PP1 binding is blocked by the Gm peptide, but not by peptides (such as Ht31) that block RII interaction with AKAPs. Protein immunoblots were done as described above with omission of the incubation with recombinant PP1.
27. PP1 activity was determined by incubating recombinant PP1 with substrate for 10 min at 30°C in the absence and presence of a purified HIS-tagged recombinant fragment of yotiao (residues 808 to 1385). Reactions were stopped by addition of trichloroacetic acid. Proteins were precipitated by centrifugation, and liberated ^{32}P was quantitated by Cerenkov counting. Reactions were performed such that the number of counts per minute liberated in the assay was ≤10% of the total cpm of substrate added to each reaction. Dose response curves for yotiao-mediated potentiation of PP1 activity toward phosphorylase *a* showed that the EC_{50} for this enhancement was 52 nM; thus, 500 nM yotiao was used in assays evaluating the effect of yotiao on NR1A dephosphorylation. Phosphorylase *a* was labeled by incubation with phosphorylase kinase; the GST-NR1A fragment was phosphorylated by PKA. Both substrates were labeled in the presence of [γ-^{32}P]ATP and then purified by ammonium sulfate precipitation and fractionation on a D-Salt Excellulose desalting column (Pierce). Labeling of GST alone demonstrated that >80% of the radioactivity was incorporated into the NR1A fragment.
28. We thank V. Coghlan and S. Olsen for isolation and analysis of the original GH4/15 clone; S. Shenolikar, C. Jahr, G. Westbrook, and colleagues at the Vollum Institute for critical evaluation of the manuscript; E. Lee for providing PP1; J. Goldenring for providing a manuscript before publicaton; and A. Westphal, K. Sandstrom, and A. Bishop for expert technical assistance. Supported in part by NIH grants NS10543 (R.S.W.), NS10202 (S.J.T.), GM 48231 (J.D.S.), and NS35050 (M.S.).

23 December 1998; accepted 1 June 1999

A Phospholipase C–Dependent Inositol Polyphosphate Kinase Pathway Required for Efficient Messenger RNA Export

John D. York,[1]* Audrey R. Odom,[1] Robert Murphy,[2] Eric B. Ives,[2] Susan R. Wente[2]*

In order to identify additional factors required for nuclear export of messenger RNA, a genetic screen was conducted with a yeast mutant deficient in a factor Gle1p, which associates with the nuclear pore complex (NPC). The three genes identified encode phospholipase C and two potential inositol polyphosphate kinases. Together, these constitute a signaling pathway from phosphatidylinositol 4,5-bisphosphate to inositol hexakisphosphate (IP_6). The common downstream effects of mutations in each component were deficiencies in IP_6 synthesis and messenger RNA export, indicating a role for IP_6 in *GLE1* function and messenger RNA export.

Spatial and temporal activation of inositol signaling pathways modulates protein machines that enable eukaryotic cells to sense changes in their environment. An essential component within this circuitry is phosphatidylinositol 4,5-bisphosphate (PIP_2), which is hydrolyzed by